www.ietdl.org

Published in IET Radar, Sonar & Navigation
Received on 12th May 2014
Revised on 2nd August 2014
Accepted on 10th August 2014
doi: 10.1049/iet-rsn.2014.0236

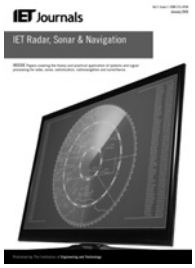

ISSN 1751-8784

Azimuth ambiguity suppression with an improved reconstruction method based on antenna pattern for multichannel synthetic aperture radar systems

Wei Wang, Robert Wang, Yunkai Deng, Wei Xu, Lei Guo, Lili Hou

Department of Space Microwave Remote Sensing System, Institute of Electronics, Chinese Academy of Sciences, Beijing, 100190, People's Republic of China
E-mail: ww_nudt@sina.com

Abstract: For synthetic aperture radar (SAR) systems, antenna array which is distributed in flight direction could increase the equivalent sample frequency in azimuth by a factor of the number of elements of antenna array. With a reconstruction algorithm, the aliased Doppler spectrum could be recovered. However, the degradation of conventional algorithms for reconstructing the Doppler spectrum with special pulse repetition frequency (PRF) shows poor robustness and the out-of-band energy which is caused by the side lobes of the antenna pattern deteriorates the azimuth ambiguity to signal ratio of a multichannel SAR. In this study, an improved reconstruction algorithm based on antenna pattern is proposed by generating an ambiguity matrix, which resembles the covariance matrix and could be used to reconstruct in-band signal and minimise the azimuth ambiguity energy. Aiming at increasing the robustness of the algorithm, the method of diagonal loading is introduced to the approach. Even in the scenario of special PRF, which is close to the singular point, the signal could be successfully reconstructed with the improved approach. Simulation results validate the proposed method.

1 Introduction

Synthetic aperture radar (SAR) is a powerful and increasingly developing technique for acquiring high-resolution radar images in all-weather conditions day and night. The applications of SAR include agriculture, ship and oil slick detection, land cover mapping, dynamic monitoring etc. [1, 2]. All those applications would benefit from high-resolution images for detailed information and from wide swath images reducing the revisiting time. However, conventional SAR systems cannot meet the two requirements simultaneously [2].

In recent years, multichannel SAR systems have been regarded as the most promising candidate for simultaneously obtaining wide swath in range and high resolution in azimuth [3–5].

In this paper, we focus on the multichannel reconstruction in azimuth. Multiple independent receiving channels arrayed in flight direction increase the number of spatial samples. Each of the receiving channel's signal is converted, digitised and stored. A digital beam forming (DBF) technique, which is called the reconstruction algorithm, can recover the Doppler spectrum even if the azimuth signal is non-uniformly sampled [6, 7]. The processing of the recorded sub-aperture signals combine the N subsampled signals to one single signal that is sampled with N PRF without aliasing. As a result, the additional samples increase the sample frequency by the factor of N. In comparison with conventional single channel SAR, multiaperture in azimuth can reduce the PRF requirement without a decrease of azimuth resolution, which offers a wider swath.

The detailed analysis of the performance of the reconstruction algorithm is presented in [3]. The performance of the reconstruction is affected, because the energy outside the band $[-N\cdot\mathrm{PRF}/2, N\cdot\mathrm{PRF}/2]$ is not cancelled by the reconstruction algorithm. The residual reconstruction error deteriorates the azimuth ambiguities. In addition, there is another problem with the conventional method. The problem is that when the PRF is close to the special PRF of the singular point, the performance of the reconstruction does degrade dramatically.

In this paper, we deal with the signals of each channel as the superposition of in-band energy and out-of-band energy based on antenna pattern. The proposed approach allows for a minimisation of the ambiguities after reconstruction. Aiming at an increased robustness of the approach, the method of diagonal loading is introduced. With the improved approach, the scenario of special PRF, which is close to the singular point, can be processed successfully.

The paper is organised as follows. The basic signal model is described in Section 2. In Section 3, the improved method for suppressing azimuth ambiguities is shown. A system design example is presented that allows for verifying the approach in Section 4. We demonstrate the performance of the proposed algorithm and compare it with the conventional algorithm. Finally, the conclusions are drawn in Section 5.

2 Signal model

We look at a multichannel SAR system with a planar antenna array consisting of N sub-antennas uniformly placed in the azimuth direction, whose geometry is shown in Fig. 1. The n_tth sub-antenna is used as the transmitting antenna and all the N sub-antennas can be used as receivers and are able to cover the illuminated area. This section introduces the signal model of the azimuth multichannel SAR system and the conventional reconstruction algorithm.

2.1 Received azimuth signals of N channels

The length of the sub-antenna is d_{az}, the distance between the phase centres of the sub-apertures is d_{az} too. Assuming that there is one point target in the swath centre and the minimal slant range between the radar and the target is R_0, the received azimuth signal [6] of the nth sub-antenna from the point target after demodulation is given by

$$u_n(\tau)=\sigma\cdot a(\theta(\tau)) \times \exp\left[-\mathrm{j}\frac{2\pi}{\lambda}\left(\sqrt{R_0^2+(V_s\tau)^2}+\sqrt{R_0^2+(V_s\tau-\Delta x_n)^2}\right)\right] \quad (1)$$

where σ represents the target reflectivity, τ is the azimuth slow time, $a(\theta(\tau))$ is the two-way antenna gain pattern, V_s represents the velocity of the radar, λ is the wavelength of the transmitted signal and $\Delta x_n=(n_t-n)\cdot d_{az}$, $n=1, 2,\ldots, N$. The n_tth channel is the transmitting channel. Using the Taylor series expansion of (1), the signal can be reformulated as

$$u_n(\tau)\simeq\sigma\cdot a\big(\theta(\tau)\big) \times \exp\left[-\mathrm{j}\frac{4\pi}{\lambda}R_0-\mathrm{j}\frac{\pi\Delta x_n^2}{2\lambda R_0}-\mathrm{j}\frac{2\pi V_s^2}{\lambda}\frac{\left(\tau-\frac{\Delta x_n}{2V_s}\right)^2}{R_0}\right] \quad (2)$$

If $n=n_t$, $u_{nt}(\tau)$ is the signal which is received by the transmitting channel and can be expressed as

$$u_{n_t}(\tau)\simeq\sigma\cdot a(\theta(\tau))\exp\left[-\mathrm{j}\frac{4\pi}{\lambda}R_0-\mathrm{j}\frac{2\pi V_s^2}{\lambda}\frac{(\tau)^2}{R_0}\right] \quad (3)$$

Compensating the second phase term of (2) with $\Phi=\exp\left[\mathrm{j}\left(\pi\Delta x_n^2/2\lambda R_0\right)\right]$ and performing the Fourier transform of $u_n(\tau)$ and $u_{nt}(\tau)$ to Doppler domain could yield

$$U_n(f)=\mathbb{F}\left[\exp\left[\mathrm{j}\frac{\pi\Delta x_n^2}{2\lambda R_0}\right]u_n(\tau)\right] \quad (4)$$

$$U_n(f)=\mathbb{F}\left[u_n(\tau)\right] \quad (5)$$

$\mathbb{F}$ represents the Fourier transformation. Comparing (2) with (3), it is easy to obtain

$$U_n(f)\simeq\exp\left(-\mathrm{j}\pi\frac{\Delta x_n}{V_s}f\right)\cdot U_{n_t}(f) \quad (6)$$

For each channel, the sample frequency of the azimuth signal is the PRF. However, B_d (Doppler bandwidth) is wider than the PRF. Therefore the sampled signal in each channel is spectrum aliasing.

If the constraint that N·PRF must be higher than B_d is satisfied, the Doppler spectrum could be recovered by the N channels' data. The existing reconstruction algorithm is based on the reconstruction of multichannel sampling of low-pass signals [8]. Many existing methods have been proposed to reconstruct the under-sampled signal [6, 7].

2.2 PRF of singular point

In Fig. 2, it is shown that with a special PRF the equivalent phase centres of the first pulse and the ones of the subsequent pulse have K coinciding points. With the introduced condition, the PRF is

$$\mathrm{PRF}=\frac{2\cdot Vs}{(N-K)\cdot d_{az}} \quad (7)$$

In this condition, the conventional reconstruction matrix would become an ill condition matrix and the conventional reconstruction algorithm would be invalid. The azimuth ambiguity to signal ratio (AASR) and the signal-to-noise ratio (SNR) influenced by the conventional reconstruction algorithm would also be worse.

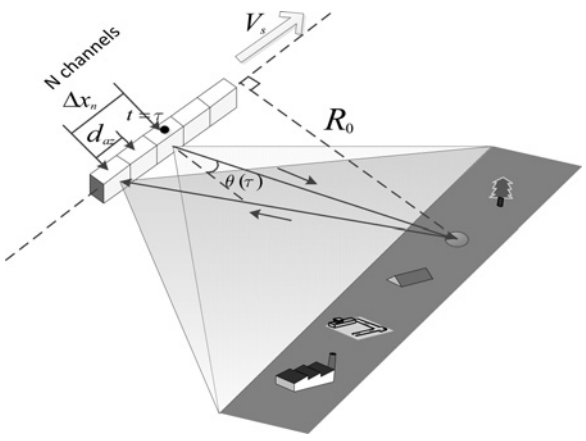

Fig. 1 *Geometry of antenna array in azimuth*

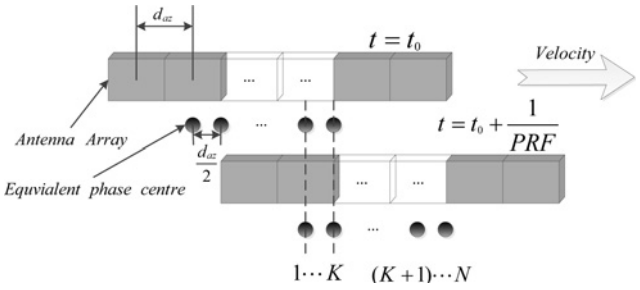

Fig. 2 *K equivalent phase centres are coincident*

3 Improved method for suppressing azimuth ambiguity

For multichannel SAR system in azimuth, the transmitting and receiving antenna pattern is shown in Fig. 3.

The azimuth signals are weighted by two-way antenna pattern, so the azimuth ambiguity energies are all brought by it. Aiming at suppressing the azimuth ambiguity signal, the in-band energy (the energy which is in the band [$-N$·PRF/2, N·PRF/2]) and out-of-band energy (the energy which is out of the band [$-N$·PRF/2, N·PRF/2]) are both considered in this section. The signal energy part and ambiguity energy part of $U_n(f)$ is shown in Fig. 4. It can be seen that the spectrum of $U_n(f)$, which is weighted by azimuth antenna pattern, is divided into several pieces with the width of the PRF. If the signal is sampled with the frequency of the PRF, the energy in all pieces would be stacked together to cause spectrum aliasing. The aliasing spectrum of $U_n(f)$ can be defined as $U_n^{\mathrm{a}}(f)$.

The energy of the frequency of f in the aliasing spectrum is a combination of all the energy of the frequency points (…, $f-2\mathrm{PRF}$, $f-\mathrm{PRF}$, f, $f+\mathrm{PRF}$, $f+2\mathrm{PRF}$, …) in the spectrum of $U_n(f)$. In Fig. 4, the frequency points are shown in Fig. 4. We clearly have (f, $f+\mathrm{PRF}$, $f+2\mathrm{PRF}$,…, $f+(N-1)\cdot\mathrm{PRF}) \in [-N\cdot\mathrm{PRF}/2, N\cdot\mathrm{PRF}/2]$.

3.1 Improved reconstruction method based on antenna pattern

Taking the received signal of the transmitting sub-antenna as the reference signal could yield

$$\begin{bmatrix} U_1^{\mathrm{a}}(f) \\ \vdots \\ U_n^{\mathrm{a}}(f) \\ \vdots \\ U_N^{\mathrm{a}}(f) \end{bmatrix} = [\ldots, \boldsymbol{\beta}_1, \boldsymbol{\beta}_2, \ldots, \boldsymbol{\beta}_N, \ldots] \cdot \begin{bmatrix} \vdots \\ U_{n_t}(f) \\ U_{n_t}(f+\mathrm{PRF}) \\ \vdots \\ U_{n_t}(f+(N-1)\cdot\mathrm{PRF}) \\ \vdots \end{bmatrix} \tag{8}$$

where $\boldsymbol{\beta}_m$ is a vector which can be expressed as

$$\boldsymbol{\beta}_m = \begin{bmatrix} \exp(-\mathrm{j}\pi(f+(m-1)\mathrm{PRF})\cdot\Delta x_1/V_s) \\ \exp(-\mathrm{j}\pi(f+(m-1)\mathrm{PRF})\cdot\Delta x_2/V_s) \\ \vdots \\ \exp(-\mathrm{j}\pi(f+(m-1)\mathrm{PRF})\cdot\Delta x_N/V_s) \end{bmatrix} \tag{9}$$

So the column number of the matrix […, $\boldsymbol{\beta}_1$, $\boldsymbol{\beta}_2$,…, $\boldsymbol{\beta}_N$, …] indicates the width of the Doppler spectrum which is considered. The spectrum of $U_n^{\mathrm{a}}(f)$ could be retrieved from each channel. The algorithm needs to reconstruct the spectrum of $U_n(f)$. In the conventional method of spatial domain, the DBF only considers the energy in the band [$-N$·PRF/2, N·PRF/2]. So in the conventional method, the energy out of the band [$-N$·PRF/2, N·PRF/2] is neglected, which means that $\boldsymbol{\beta}_m(m \in [1,\ldots,N])$ and $U_{n_t}(f)\big(f \notin [-N\cdot\mathrm{PRF}/2, N\cdot\mathrm{PRF}/2]\big)$ are not taken into account. In the conventional method, we could find a weight vector $\boldsymbol{w}_k = [\omega_{k1}, \omega_{k2},\ldots,\omega_{kN}]$ which satisfies

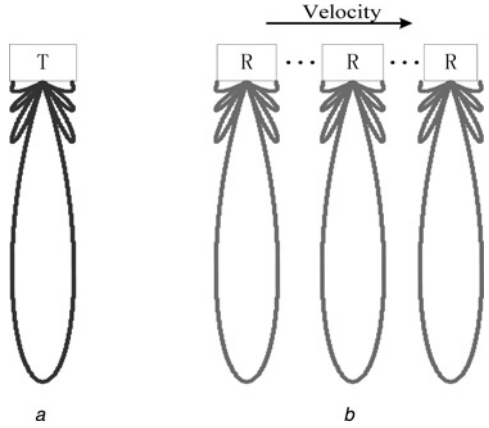

Fig. 3 *Azimuth transmitting and receiving antenna pattern*
a Transmitting antenna pattern
b Receiving antenna pattern of each sub-antenna

$$\boldsymbol{w}_k \cdot \begin{bmatrix} U_1^{\mathrm{a}}(f) \\ \vdots \\ U_n^{\mathrm{a}}(f) \\ \vdots \\ U_N^{\mathrm{a}}(f) \end{bmatrix} = [\omega_{k1}, \ldots, \omega_{kn}, \ldots, \omega_{kN}] \cdot \begin{bmatrix} U_1^{\mathrm{a}}(f) \\ \vdots \\ U_n^{\mathrm{a}}(f) \\ \vdots \\ U_N^{\mathrm{a}}(f) \end{bmatrix} = U_{n_t}(f+(k-1)\cdot\mathrm{PRF}) \tag{10}$$

Substituting (8)–(10), we obtain

$$\boldsymbol{w}_k \cdot [\boldsymbol{\beta}_1, \ldots \boldsymbol{\beta}_k, \ldots, \boldsymbol{\beta}_N] = [0, \ldots, 1, \ldots, 0] \tag{11}$$

Therefore the reconstruction weights of the conventional

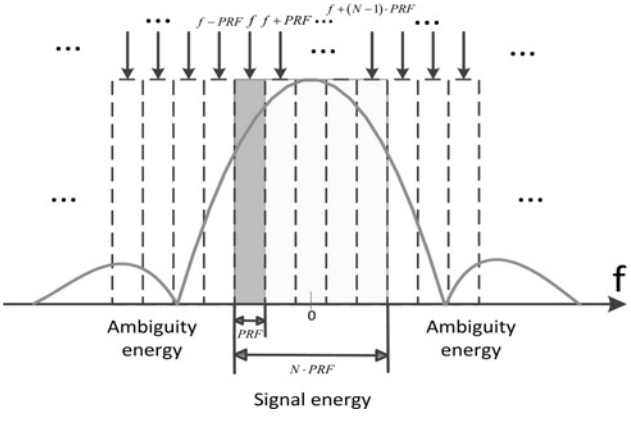

Fig. 4 *Spectrum of $U_n(f)$ weighted by azimuth antenna pattern*

doi: 10.1049/iet-rsn.2014.0236

method are

$$\begin{bmatrix} \boldsymbol{w}_1 \\ \vdots \\ \boldsymbol{w}_k \\ \vdots \\ \boldsymbol{w}_N \end{bmatrix} = \left[\boldsymbol{\beta}_1, \ldots \boldsymbol{\beta}_k, \ldots, \boldsymbol{\beta}_N\right]^{-1} \tag{12}$$

However, in real scenes, the azimuth spectrum is not band limited. Therefore, if considering the energy out of the band $[-N\cdot\mathrm{PRF}/2, N\cdot\mathrm{PRF}/2]$ and using the reconstruction filter in (12) to recover the spectrum, all the energy outside the band $[-N\cdot\mathrm{PRF}/2, N\cdot\mathrm{PRF}/2]$ would deteriorate the AASR. Using $\boldsymbol{w}_k$ to reconstruct $U_{nt}(f+(k-1)\cdot\mathrm{PRF})$ could yield

$$\begin{aligned} \boldsymbol{w}_k \cdot \begin{bmatrix} U_1^{\mathrm{a}}(f) \\ \vdots \\ U_n^{\mathrm{a}}(f) \\ \vdots \\ U_N^{\mathrm{a}}(f) \end{bmatrix} &= \boldsymbol{w}_k \cdot \left[\ldots, \beta_1, \beta_2, \ldots, \beta_N, \ldots\right] \\ &\cdot \begin{bmatrix} \vdots \\ U_{n_t}(f) \\ U_{n_t}(f+\mathrm{PRF}) \\ \vdots \\ U_{n_t}(f+(N-1)\cdot\mathrm{PRF}) \\ \vdots \end{bmatrix} \\ &= \left[\sum_{m\neq k} \boldsymbol{w}_k \cdot \boldsymbol{\beta}_m \cdot U_{n_t}(f+(m-1)\cdot\mathrm{PRF})\right] \\ &\quad + U_{n_t}(f+(k-1)\cdot\mathrm{PRF}) \end{aligned} \tag{13}$$

$U_{nt}(f+(k-1)\cdot\mathrm{PRF})$ is the signal which is reconstructed, and the ambiguous signal is $\sum_{m\neq k} \boldsymbol{w}_k \cdot \boldsymbol{\beta}_m \cdot U_{n_t}(f+(m-1)\cdot\mathrm{PRF})$. so the power of ambiguity energy could be written as

$$P_{\mathrm{AM}}(k) = \sum_{m\neq k} \left|\boldsymbol{w}_k \cdot \boldsymbol{\beta}_m \cdot U_{n_t}(f+(m-1)\cdot\mathrm{PRF})\right|^2 \tag{14}$$

The goal of this paper is to find an improved weight vector $\boldsymbol{w}'_k$ to reconstruct the in-band energy and minimise the ambiguity energy. If

$$\boldsymbol{w}'_k \cdot \boldsymbol{\beta}_k = 1 \tag{15}$$

After reconstruction, the energy of ambiguity is

$$P'_{\mathrm{AM}}(k) = \sum_{m\neq k} \left|\boldsymbol{w}'_k \cdot \boldsymbol{\beta}_m \cdot U_{n_t}(f+(m-1)\cdot\mathrm{PRF})\right|^2 \tag{16}$$

$P'_{\mathrm{AM}}(k)$ can be reformulated as (17).
Defining

$$\boldsymbol{R}_k = \left(\sum\nolimits_{m\neq k} \left[\left|U_{n_t}(f+(m-1)\cdot\mathrm{PRF})\right|^2 \cdot \left(\boldsymbol{\beta}_m \cdot \boldsymbol{\beta}_m^{\mathrm{H}}\right)\right]\right)$$

$\boldsymbol{R}_k$ is a matrix similar to a covariance matrix.

Assuming that $a(\theta)$ is known as the two-way antenna gain pattern of the radar. As the amplitude of the Doppler spectrum has the same shape with the antenna pattern, so we have

$$\left|U_{n_t}(f+(m-1)\cdot\mathrm{PRF})\right|^2 = \alpha \cdot \left|a[\theta(f+(m-1)\cdot\mathrm{PRF})]\right|^2 \tag{18}$$

α is a constant. Combining (15) and (17), the weight vector has to satisfy

$$\begin{cases} \boldsymbol{w}'_k \cdot \boldsymbol{\beta}_k = 1 \\ \min\limits_{\boldsymbol{w}'_k} \left(P'_{\mathrm{AM}}(k)\right) \end{cases} \tag{19}$$

Based on the method of Lagrange multipliers, the solution of (19) is

$$\boldsymbol{w}_k'^{\mathrm{H}} = \frac{\boldsymbol{R}_k^{-1}\boldsymbol{\beta}_k}{\boldsymbol{\beta}_k^{\mathrm{H}}\boldsymbol{R}_k^{-1}\boldsymbol{\beta}_k} \tag{20}$$

The result is similar to the minimum variance distortionless response (MVDR) algorithm [9]. With the proposed $\boldsymbol{w}'_k$, the Doppler spectrum can be reconstructed and the ambiguity energy is suppressed. For the Doppler spectrum being wider than $N\cdot\mathrm{PRF}$, the proposed method is using $N-1$ degrees of freedom to suppress more than $N-1$ ambiguous energy and could minimise the total remaining ambiguous energy.

For minimising the total azimuth ambiguous energy, all the signals out of the band should be considered. However, the number of frequency slots cannot be set arbitrary large, because the maximum of the Doppler bandwidth is $(2V_s/\lambda)(\sin(\pi/2)-\sin(-\pi/2)) = (4V_s/\lambda)$. So the maximum number of slots is the integer part of $(4V_s/\pi)/\mathrm{PRF}$. However, in real scenes, we know that the outer parts of side lobes of antenna beam pattern are low and make little contributions to azimuth ambiguous energy, so there is no need to calculate all the frequency slots. For better performance and making the proposed method efficient, the minimum number of frequency slots should be chosen with a rational value based on the calculated AASR of the multichannel system.

Since the purpose of the proposed method is to get an improved reconstruction filter, the performance analysis procedure in [3, 10] is suitable for the improved algorithm.

For multichannel system, the influence of reconstruction filter to SNR is derived in [3, 10] with a measure for the

$$\begin{aligned} P'_{\mathrm{AM}}(k) &= \sum_{m\neq k} \left[w'_k \cdot \boldsymbol{\beta}_m \cdot U_{n_t}(f+(m-1)\cdot\mathrm{PRF})\right] \cdot \left[\boldsymbol{w}'_k \cdot \boldsymbol{\beta}_{\boldsymbol{m}} \cdot U_{n_t}(f+(m-1)\cdot\mathrm{PRF})\right]^{\mathrm{H}} \\ &= \boldsymbol{w}'_k \left(\sum_{m\neq k} \left[\left|U_{n_t}(f+(m-1)\cdot\mathrm{PRF})\right|^2 \cdot \left(\boldsymbol{\beta}_m \cdot \boldsymbol{\beta}_m^{\mathrm{H}}\right)\right]\right) w_k'^{\mathrm{H}} = \boldsymbol{w}'_k \boldsymbol{R}_k \boldsymbol{w}_k'^{\mathrm{H}} \end{aligned} \tag{17}$$

image. The influence factor named SNR scaling is defined as

$$\Phi_{bf,B_D} = N \cdot \sum_{j=1}^{N} E\left[\left|P_j(f)\right|^2 \cdot \mathrm{rect}\left(\frac{f}{B_D}\right)\right] \tag{21}$$

where $P_j(f)$ is the reconstruction filter of the jth channel. In Section 4, the AASR and the SNR scaling of the proposed approach are analysed and compared with the conventional method.

3.2 Processing with special PRF of singular point

Assuming $K(1 \le K < N)$ overlapped equivalent phase centres with PRF = $(2 \cdot Vs/(N-K) \cdot d_{az})$ and m is an integer, we have (22).

So $\boldsymbol{\beta}_m$ and $\boldsymbol{\beta}_{N-K+m}$ are linear dependent. The rank of $\left[\boldsymbol{\beta}_m \ \cdots \ \boldsymbol{\beta}_{m+N-1}\right]$ is $(N-K)$. The matrix $\boldsymbol{R}_k$ can be rewritten as

$$\boldsymbol{R}_k = \left[\ldots \boldsymbol{\beta}_1 \ \cdots \ \boldsymbol{\beta}_N \ldots\right] \cdot \begin{bmatrix} \vdots \\ \left|U_{n_t}(f)\right|^2 \boldsymbol{\beta}_1^{\mathrm{T}} \\ \vdots \\ \left|U_{n_t}(f+(N-1)\mathrm{PRF})\right|^2 \boldsymbol{\beta}_N^{\mathrm{T}} \\ \vdots \end{bmatrix} \tag{23}$$

Therefore the rank of $\boldsymbol{R}_k$ is less than N. To use the proposed reconstruction, the method of diagonal loading [9] is exploited to solve the matrix's morbidity.

A new matrix is defined as

$$\boldsymbol{R}_{kl} = \boldsymbol{R}_k + \sigma_{\mathrm{L}}^2 \boldsymbol{I} \tag{24}$$

where σ_{L}^2 is the loading factor of the matrix $\boldsymbol{R}_k$.

Substituting (24) into (20)

$$\boldsymbol{w}_k'^{\mathrm{H}} = \frac{\boldsymbol{R}_{kl}^{-1}\boldsymbol{\beta}_k}{\boldsymbol{\beta}_k^H \boldsymbol{R}_{kl}^{-1}\boldsymbol{\beta}_k} \tag{25}$$

From (22), we obtain that

$$\begin{aligned} &\boldsymbol{w}_m'^{\mathrm{H}} \cdot \boldsymbol{\beta}_{N-K+m} \cdot \boldsymbol{\beta}_{N-K+m}^{\mathrm{H}} \cdot \boldsymbol{w}_m' \\ &= \boldsymbol{w}_m'^{\mathrm{H}} \cdot \boldsymbol{\beta}_m \cdot \boldsymbol{\beta}_m^{\mathrm{H}} \cdot \boldsymbol{w}_m' = 1 \end{aligned} \tag{26}$$

$$\begin{aligned} &\boldsymbol{w}_{N-K+m}'^{\mathrm{H}} \cdot \boldsymbol{\beta}_{N-K+m} \cdot \boldsymbol{\beta}_{N-K+m}^{\mathrm{H}} \cdot \boldsymbol{w}_{N-K+m}' \\ &= \boldsymbol{w}_{N-K+m}'^{\mathrm{H}} \cdot \boldsymbol{\beta}_m \cdot \boldsymbol{\beta}_m^{\mathrm{H}} \cdot \boldsymbol{w}_{N-K+m}' = 1 \end{aligned} \tag{27}$$

Therefore, the Doppler spectrum at the frequency point of $f+(m-1)\cdot\mathrm{PRF}$ and $f+(N-K+m-1)\cdot\mathrm{PRF}$ cannot be reconstructed simultaneously. So the proposed method could reconstruct the signal inside the band $[-(N-K)\cdot\mathrm{PRF}/2, (N-K)\cdot\mathrm{PRF}/2]$ and the bandwidth is $(N-K)\cdot\mathrm{PRF} = (2Vs/d_{az})$. However, the signal outside the band $[-(N-K)\cdot\mathrm{PRF}/2, (N-K)\cdot\mathrm{PRF}/2]$ cannot be reconstructed successfully. So after processing the Doppler spectrum with our proposed approach, the signal inside the band $[-(N-K)\cdot\mathrm{PRF}/2, (N-K)\cdot\mathrm{PRF}/2]$ is the reconstructed azimuth signal which is needed. For recovering the signal, the Doppler bandwidth of the system must be narrower than $(N-K)\cdot\mathrm{PRF}$. However, there is residual energy out of the bandwidth $[-(N-K)\cdot\mathrm{PRF}/2, (N-K)\cdot\mathrm{PRF}/2]$ after reconstruction. To solve this problem, a low-pass filter $H_{\mathrm{lp}}(f)$ is introduced as

$$H_{\mathrm{lp}}(f) = \mathrm{rect}\left(\frac{f}{B_{\mathrm{dop}}}\right) \tag{28}$$

In addition, when the PRF is close to the special PRF of the singular point, the matrix $\boldsymbol{R}_k$ would be morbid too. Under this circumstance, the proposed approach is still valid.

4 Numerical simulation results

To validate the performance and the properties of the developed reconstruction method, the following cases are considered: the first is the reconstruction of the azimuth signal, which is non-uniformly sampled (not with the PRF of the singular point); the second is to analyse the AASR of

Table 1 SAR system parameters

orbit height	700 km
radar velocity	7508 m/s
wavelength	0.0555 m
Doppler bandwidth	6648.6 Hz
length of the whole antenna	10 m
number of channels in azimuth	5
length of receiving sub-antenna	2 m
receive aperture spacing	2 m
length of transmitting antenna	2 m
slant range of the point target	900 km
uniform PRF	1501.6 Hz

$$\begin{aligned} \boldsymbol{\beta}_{N-K+m} &= \begin{bmatrix} \exp\left(-\mathrm{j}\pi\left(f+(N-K+m-1)\mathrm{PRF}\right)\cdot\Delta x_1/V_s\right) \\ \exp\left(-\mathrm{j}\pi\left(f+(N-K+m-1)\mathrm{PRF}\right)\cdot\Delta x_2/V_s\right) \\ \vdots \\ \exp\left(-\mathrm{j}\pi\left(f+(N-K+m-1)\mathrm{PRF}\right)\cdot\Delta x_N/V_s\right) \end{bmatrix} \\ &= \begin{bmatrix} \exp\left(-\mathrm{j}\pi(f+(m-1)\mathrm{PRF})\cdot\Delta x_1/V_s\right) \\ \exp\left(-\mathrm{j}\pi(f+(m-1)\mathrm{PRF})\cdot\Delta x_2/V_s\right) \\ \vdots \\ \exp\left(-\mathrm{j}\pi(f+(m-1)\mathrm{PRF})\cdot\Delta x_N/V_s\right) \end{bmatrix} \cdot \exp\left(-\mathrm{j}\pi(N+1)\right) \\ &= \boldsymbol{\beta}_m \cdot \exp\left(-\mathrm{j}\pi(N+1)\right) \end{aligned} \tag{22}$$

doi: 10.1049/iet-rsn.2014.0236

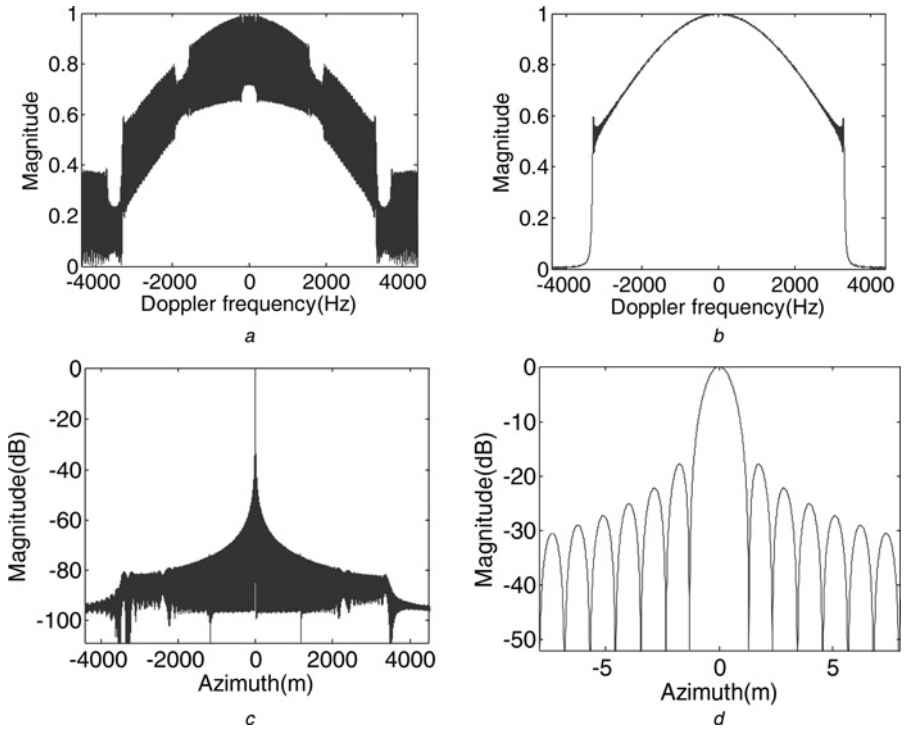

Fig. 5 *Reconstruction of the signal with PRF = 1751 Hz*

a Doppler spectrum before reconstruction
b Reconstructed spectrum
c Compressed signal after reconstruction
d Zoom in the compressed signal

the signal with out-of-band energy; the third is to analyse the performance of the processing with the PRF of the singular point; the fourth, the SNR scaling of the proposed approach is calculated. At last, an example with non-uniform physical spacing channels is simulated.

In the simulation, one target in the swath centre is assumed. The designed system parameters are listed in Table 1.

4.1 Reconstruction of the in-band Doppler spectrum

In this section, the reconstruction of the in-band Doppler spectrum is simulated using the proposed algorithm.

The uniformity factor can be defined by $F_{un} = \mathrm{PRF}/\mathrm{PRF}_{uni}$. In this section, a PRF of 1751 Hz is simulated. Therefore the uniformity is 1.17. From Fig. 5, it can be seen that the approach shows a good performance in reconstructing the in-band Doppler spectrum.

4.2 Performance of suppressing AASR

In this section, the AASR of the SAR system with conventional reconstruction method and the proposed method are calculated. In Fig. 6, the solid line shows the AASR of the multichannel signal reconstructed with the conventional method and the dashed line shows the AASR of an equivalent system with single channel (equivalent system with single channel means one-channel SAR system with azimuth sample frequency of N·PRF and that all other parameters are identical to the multichannel system).

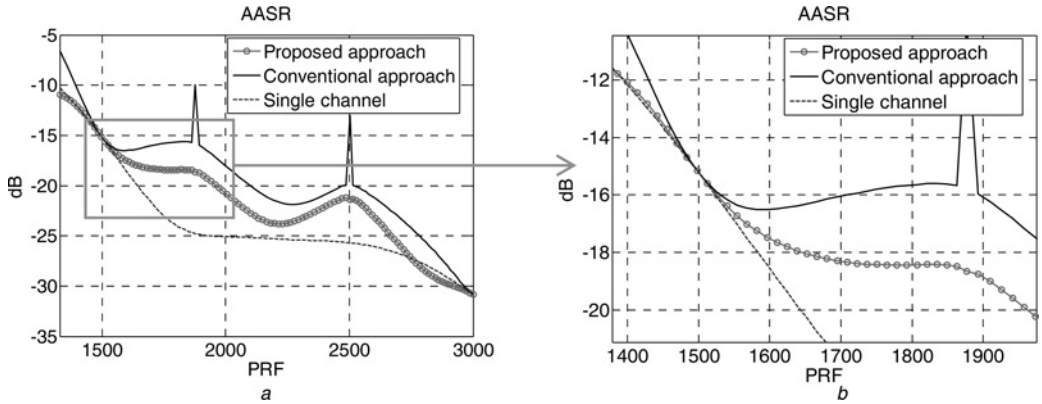

Fig. 6 *AASR of the system with conventional method (solid line), proposed method (circle) and the AASR of equivalent system with one channel (dashed line)*

a Simulated AASR of the system
b The AASR of the system with the PRFs around the uniform PRF

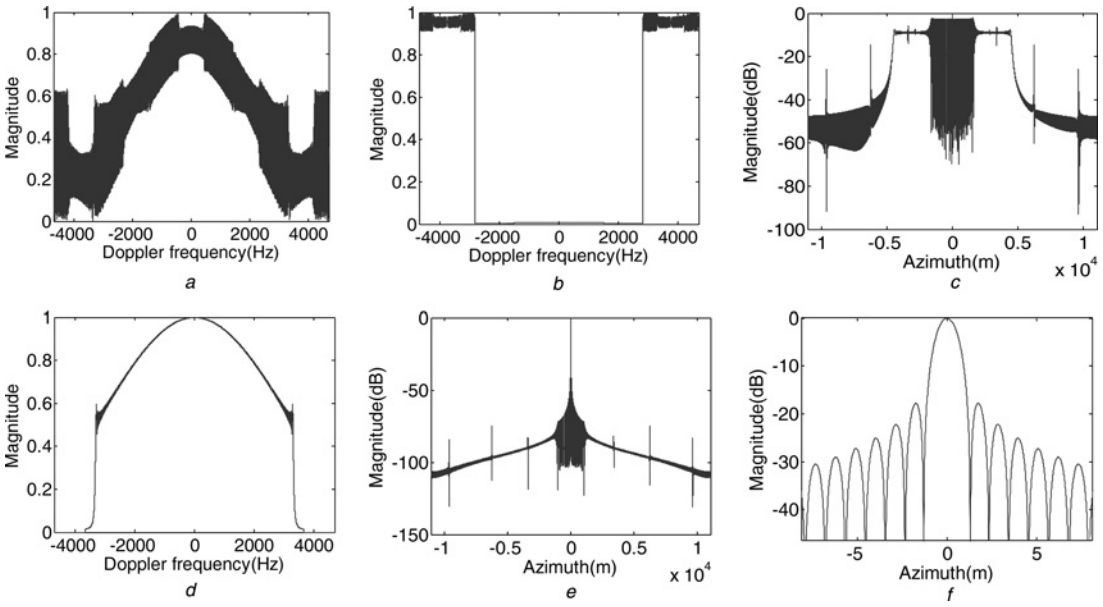

Fig. 7 *Reconstruction with the special PRF (1876 Hz) of singular point*

a Aliased spectrum
b Reconstructed by conventional method
c Compressed signal of *b*
d Reconstructed by proposed method
e Compressed signal of *d*
f Zoom in the compressed signal in *e*

Examining Fig. 6, it can be seen that the AASR of the multichannel system is much worse than the equivalent system with one channel. The two AASR are equal at the PRF of 1501.6 Hz, because the azimuth signal is uniformly sampled at this PRF. The AASR of multichannel system with the proposed algorithm is shown with circles. It can be seen that the AASR of the proposed method is better than the conventional one.

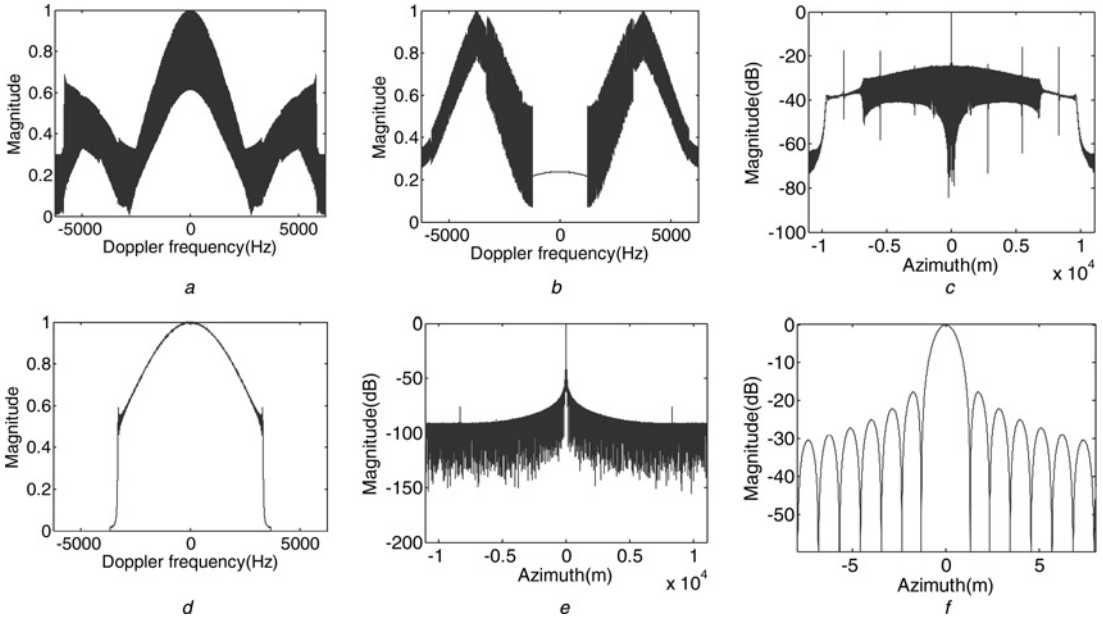

Fig. 8 *Reconstruction with the PRF (2503 Hz) close to singular point*

a Aliased spectrum
b Reconstructed by conventional method
c Compressed signal of *b*
d Reconstructed by proposed method
e Compressed signal of *d*
f Zoom in the compressed signal in *e*

doi: 10.1049/iet-rsn.2014.0236

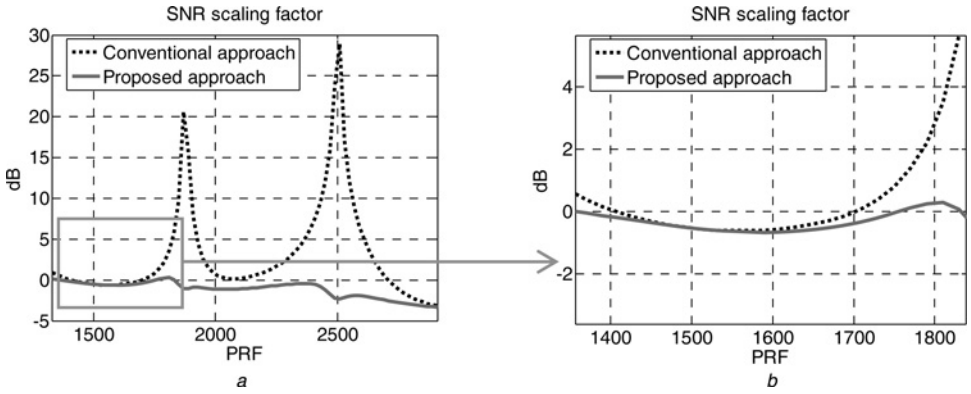

Fig. 9 *SNR scaling factor of conventional and proposed methods*

a Simulated SNR scaling factor of the system
b The SNR scaling factor of the system with the PRFs around the uniform PRF

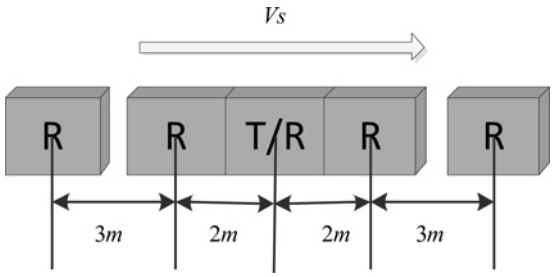

Fig. 10 *Structure of the non-uniform spacing antennas*

4.3 Reconstruction performance with the PRF close to the singular point

First, the reconstruction performance with the PRF of the singular point is analysed. For example, when PRF = $2V_s/((N-1)\cdot d_{az})$ = 1876 Hz, the last equivalent phase centre of the first pulse is overlapping with the first equivalent phase centre of the subsequent pulse. From Fig. 7, it can be seen that the conventional reconstruction is invalid. However, with the proposed method the signal is reconstructed successfully.

Then, the performance of the approach with PRF close to the singular point, which causes two equivalent phase centres' coincidence, is analysed. The singular point is $2V_s/((N-2)\cdot d_{az})$=2501 Hz, so the PRF = 2503 Hz is chosen, the

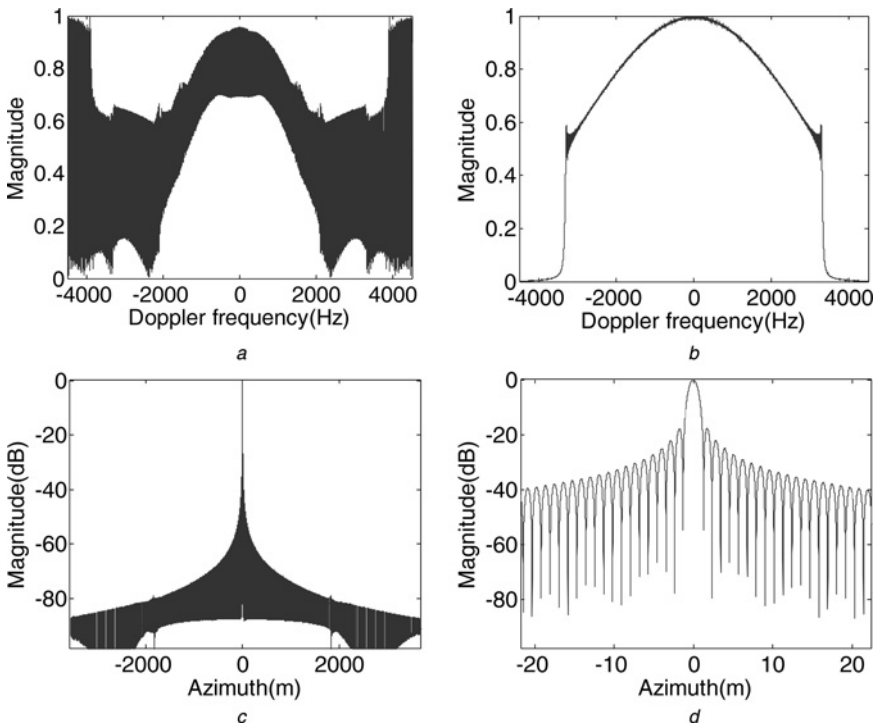

Fig. 11 *Reconstruction of the signal with PRF = 1800 Hz for non-uniform spacing antenna*

a Doppler spectrum before reconstruction
b Reconstructed spectrum
c Compressed signal after reconstruction
d Zoom in the compressed signal

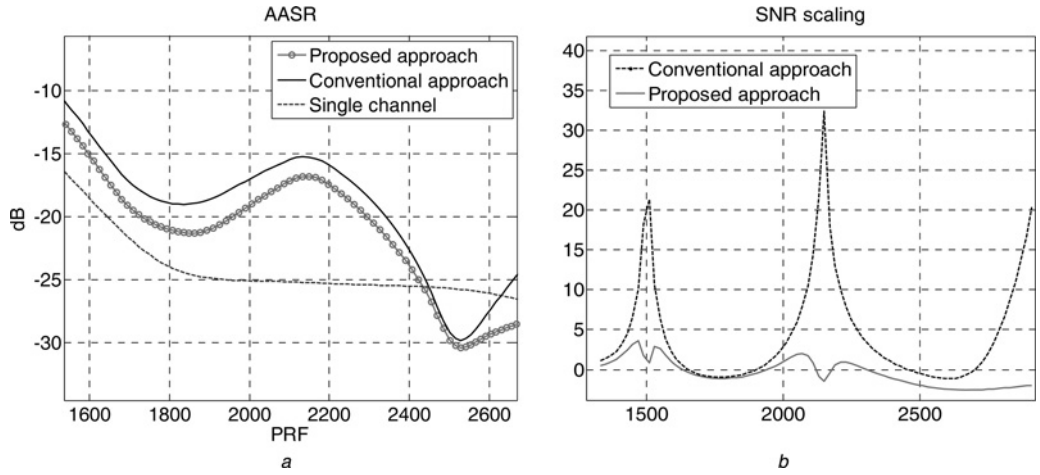

Fig. 12 *Simulated performance of the system with non-uniform space antenna*

a AASR of the non-uniform space antenna system with conventional and proposed methods
b SNR scaling factor of the non-uniform space antenna system with conventional and proposed methods

reconstruction result is shown in Fig. 8. It is clear that the proposed method shows better robustness.

4.4 SNR scaling with the proposed method

The SNR scaling factor is calculated in this section. In Fig. 9, the dashed line shows the SNR scaling factor of the conventional method, the solid line shows the one of the proposed approach. It can be seen that with the proposed approach, a better SNR scaling is obtained for all tested PRF values. The two factors are equal at the PRF of 1501.6 Hz, because the azimuth signal is uniformly sampled at this PRF.

4.5 Simulation with non-uniform spacing channels

It is clear that the multichannel in azimuth is substantial to get periodically non-uniform sampling of azimuth signals. If the azimuth antennas are non-uniform spacing in azimuth, the signal received by non-uniform spacing antennas is periodically non-uniform sampling signal too. For evaluating the proposed approach with non-uniform spacing channels, we should analyse this condition in this section. In this condition, Δx_n cannot satisfy the equation $\Delta x_n = (n_t - n)\cdot d_{az}$. However, this symbol Δx_n still can be used for representing the distance between the nth receiving sub-antenna and the transmitting antenna centre. All the other derivations are the same with the uniform spacing condition.

A system example is simulated. In this simulation, the structure of the antenna is in Fig. 10.

The system parameters are the same with the parameters in Table 1. Fig. 11 shows the reconstruction result using the proposed approach.

From the Fig. 11, it can be seen that the Doppler spectrum is reconstructed successfully.

The AASR and SNR scaling factor of the system with non-uniform space antenna is in Fig. 12. The figures in Fig. 12 show that the proposed approach also has better performance than the conventional one with the condition of non-uniform spacing of the sub-antennas.

5 Conclusion

This paper presents an improved reconstruction approach for multichannel SAR in azimuth to suppress the ambiguity energy after reconstruction. A matrix that is similar to the covariance matrix is generated for finding an optimal solution to reconstruct the Doppler spectrum and minimising the ambiguous energy based on antenna pattern. To get better robustness, the method of diagonal loading is used. Simulation results show that the proposed approach offers better AASR, better robustness and better SNR scaling than the conventional one. Therefore, the proposed approach can promote the applications of multichannel SAR in azimuth for the development and implementation of a new generation of more powerful SAR systems and missions.

6 References

1 Henderson, F., Lewis, A.: 'Manual of remote sensing: principles and applications of imaging radar' (Wiley, New York, 1998)
2 Curlander, J.C., McDonough, R.N.: 'Synthetic aperture radar, systems and signal processing' (John Wiley & Sons Inc., New York, 1991)
3 Gebert, N., Krieger, G., Moreira, A.: 'Digital beam forming on receive: techniques and optimization strategies for high-resolution and wide-swath SAR imaging', *IEEE Trans. Aerosp. Electron. Syst.*, 2009, **45**, (2), pp. 564–592
4 Younis, M., Huber, S., Patyuchenko, A., Bordoni, F.: 'Performance comparison of reflector- and planar-antenna based digital beam-forming SAR', *Int. J. Antennas Propag.*, 2009, **2009**, pp. 1–13
5 Krieger, G., Gebert, N., Moreira, A.: 'Multidimensional waveform encoding: a new digital beamforming technique for synthetic aperture radar remote sensing', *IEEE Trans. Geosci. Remote Sens.*, 2008, **46**, (1), pp. 31–46
6 Krieger, G., Fiedler, H., Rodriguez-Cassola, M., Hounam, D., Moreira, A.: 'System concepts for bi- and multistatic SAR missions'. Proc. ASAR Workshop 2003, Saint-Hubert, Quebec, Canada, June 2003, pp. 331–339
7 Krieger, G., Gebert, N., Moreira, A.: 'SAR signal reconstruction from non-uniform displaced phase center sampling'. Proc. Int. Geoscience and Remote Sensing Symp. (IGARSS), Alaska, USA, September 2004, pp. 1763–1766
8 Brown, J.L.: 'Multi-channel sampling of low-pass signals', *IEEE Trans. Circuits Syst.*, 1981, **28**, (2), pp. 101–106
9 Van Trees, H.L.: 'Optimum array processing: detection, estimation, and modulation theory, Part IV' (John Wiley & Sons, New York, 2002)
10 Gebert, N.: 'Multi-channel azimuth processing for high-resolution wide-swath SAR imaging'. DLR-Forschungsbericht. DLR-FB 2009-13, 215 S

doi: 10.1049/iet-rsn.2014.0236